Identification and Classification of Selected Internal Combustion Engine Inefficiency Based on Vehicle Structure Vibrations

Krzysztof PRAŻNOWSKI, Jarosław MAMALA,
Andrzej BIENIEK, Mariusz GRABA
Opole University of Technology, Mechanical Department,
Mikołajczyka street 5, 45-271 Opole,
k.praznowski@po.edu.pl, j.mamala@po.edu.pl,
a.bieniek@po.edu.pl, m.graba@po.edu.pl

Abstract

The combustion engine generates forced vibrations, caused by periodically acting external forces resulting from the combustion of the fuel-air mixture. Any changes in this process cause an increase in the value of vibration amplitude and a change in the distribution of harmonics dominating in the frequency domain. In order to identify selected malfunctions of the internal combustion engine of the Polaris off-road vehicle tested, its current parameters were correlated with the vibrations transmitted to the vehicle's structural elements. An integrated sensor for measuring acceleration using the direct method, made in MEMS technology, was used for the tests.

The recorded signals of the acceleration components were subjected to analysis in the frequency domain, thus identifying the characteristic harmonic components in the analyzed spectrum. For the classification of incompleteness based on registered signals, a diagnostic inference matrix based on our own algorithm of conduct was used.

Keywords: short-term analysis, Fourier transform, engine diagnostics, diagnostic matrix

1. Introduction

In most internal combustion engines, fuel combustion occurs between the piston, cylinder and head. Then we deal with internal combustion engines in which mechanical work is carried out in a periodically repeatable manner and dependent on the number of strokes and the angular speed of the engine crankshaft [1]. The course of the fuel-air mixture combustion process in this type of engines is very intense at significant variable combustion pressures, which contributes to the formation of large energy pulses affecting the crank-piston system changing the instantaneous crankshaft angular velocity. The analysis of the instantaneous change in the angular velocity of the engine crankshaft was used to detect combustion process irregularities [2]. The phenomenon of disturbed combustion process of the mixture is also visible when applying direct pressure measurement in the combustion chamber. This manifests itself then in the oscillation of the pressure in the combustion chamber [3, 4]. However, the method is limited due to low durability and high cost of implementation.

Another method of diagnosing the correctness of combustion of the fuel-air mixture in the engine is the vibration analysis of the internal combustion engine [5-10]. In internal combustion engines, the detection of this process uses both the measurement of the angular speed of the crankshaft of the engine, by using a speed with higher

resolution correlated with the knock sensor. This combination is due to the large number of factors that affect the knock sensor vibration measurement process. This process may be preceded by signal re-sampling [11] and deeper spectral analysis allowing obtaining a spectrum with a characteristic harmonic component. Acceleration value recorded at the output of the acceleration sensor mounted on the engine body, represent the processed response of the elastic system to forced type: pressure changes as a result of combustion, pulsation of exhaust gases in the exhaust duct, etc. In addition, the measurement of body vibrations and analysis of statistical features is used to assess the impact of various fuels (gasoline, ethanol) for the correct implementation of the combustion process in the engine [4].

In [12] the application of the classification algorithm based on artificial neural networks (ANN), carrier vector machines (SVM) and k Neighbor Neighbor (kNN) classification algorithms are employed to predict if the motor works healthily based on the selected features and, if not what kind of faults is in the engine.

However, during operation of an internal combustion engine, its emergency conditions may occur resulting in introducing the engine into uncontrolled disturbances in its operation. This phenomenon may result, for example, from a malfunctioning fuel injection system. The resulting malfunction of the engine in the form of shutting down the cylinder from work causes a change in the amplitude spectrum of engine body accelerations.

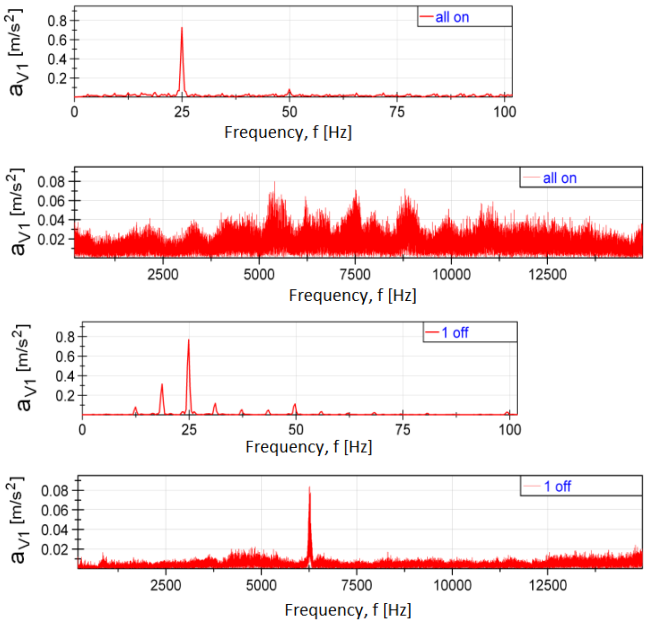

Figure. 1. Frequency spectrum of the vertical vibration acceleration – 1st cyl. [9]

As presented in [9], switching off one of the cylinders reduces the value of the amplitude of the engine vibration acceleration in both directions for all frequencies from

2.5 to 15 kHz except for the frequency of about 6.25 kHz, which is visible in the characteristic increase in amplitude in the spectrum of the tested signal. However, changes in the low frequency range (fundamental frequency and its multiplicity) were found. The harmonic increase occurs when one (several Fig. 1) or several cylinders are turned off.

The resulting vibrations of the engine and other elements of the chassis are transmitted by the engine mounting elements to the vehicle body [10]. The elastically damping properties of these elements are selected so that the occurring vibrations are the least burdensome for the vehicle user and do not cause stress in the body structure. However, these vibrations can be a source of diagnostic information [13, 14] about the occurrence of an internal combustion engine malfunction resulting from an incorrect combustion process. This information constituted the basis for undertaking works related to the identification of a combustion engine malfunction based on vibrations of the vehicle structure. Such a solution can be used in the conditions of actual operation to infer about the technical condition of selected components of the propulsion system [15].

2. Research object

The research involved the use of a Polaris off-road vehicle, which was equipped with an original integrated measuring system consisting of a wireless data transmission system from the on-board CAN BUS network and an acceleration sensor (Fig. 1). The wireless data transmission system uses diagnostic connector signals and allows data to be transferred from the vehicle to the recording computer using a radio transmitter operating in the 433 MHz band, which range is up to 1 km.

The sensor (3DM-GX3-25) was used to measure acceleration by a direct method. It is made in MEMS technology. The sensor is insensitive to the effects of internal noise of conditioning systems due to the use of a set of sensors with pulse PWM output. It has a built-in processor, which thanks to the algorithm of measurement synthesis provides static and dynamic orientation of its measurement axes. Basic parameters of the sensor are given in Table 1.

Table 1. Parameters of the sensor 3DM-GX3-25

Quantity	Value
Attitude heading range	360° about all 3 axes
Accelerometer range	±5g standard
Gyroscope range	±300°/sec standard
Static accuracy	±0.5° pitch, roll, heading typical for static test conditions
Data output rate	up to 1000 Hz
Filtering	sensors sampled at 30 kHz, digitally filtered (user adjustable) and scaled into physical units; coning and sculling integrals computed at 1 kHz
Interface	RS232
Baud rate	115,200 bps to 921,600 bps
Power supply voltage	+3.2 to +16 volts DC

The sensor was mounted on a structural element (frame) of the tested vehicle. This solution is intended to determine the possibility of using the vibrations of the support structure to identify selected given internal combustion engine malfunctions. The elastic damping elements fixing the engine to the frame did not show any operational damage. Directional setting of the sensor axis for recording vibrations caused by the operating internal combustion engine relative to the engine crankshaft: x – longitudinal axis, y – transverse axis, z – vertical axis is shown in Fig. 2.

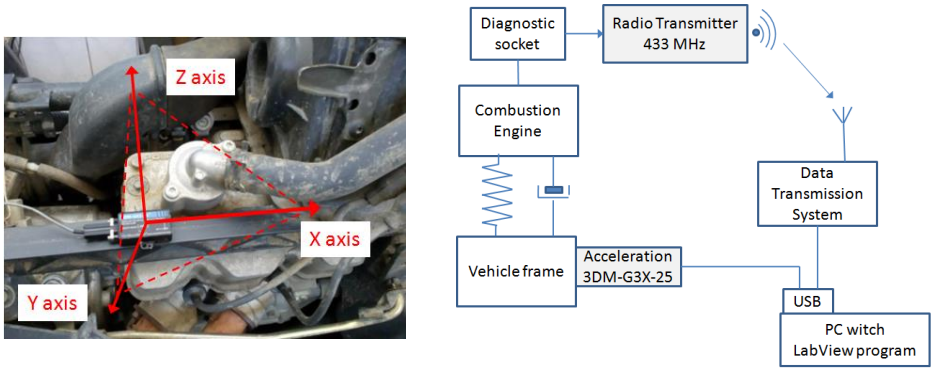

Figure 2. Placement of the 3DM-GX3-25 sensor on the vehicle during tests and block diagram of the measuring system

3. Signal analysis

The own application developed in MATLAB was used to analyze the recorded acceleration sensor signal and engine operating parameters. Due to the diversity of signal sampling (866 Hz for acceleration sensor and 132 Hz for engine running signal), the signals were synchronized.

The recorded signal from the acceleration sensor was analyzed using the Short-Term Fourier Transform (STFT) method. In the first phase, the STFT method consists in dividing the input signal into smaller segments, in which it can be treated as quasi-stationary, and then processing it based on the FFT algorithm of individual data segments. Short-term Fourier transform is described by equation 1, while the input signal is equated by equation 2.

$$STFT[x_w(t,\tau)] = \int_{-\infty}^{\infty} w(t,\tau)x(t)e^{-j2\pi ft}dt \tag{1}$$

$$x_w(t,\tau) = w(t,\tau)x(t) \tag{2}$$

In this way, a frequency and spectral map of the analyzed vehicle body vibration signal was obtained as a result of forcing the operating internal combustion engine (Fig. 3, 4, 5).

The obtained waveforms showed the occurrence of clear amplitudes in the range of the fundamental frequency f_1, as well as its subsequent harmonic order ($f_{0.5}$, $f_{1.5}$, f_2, $f_{2.5}$).

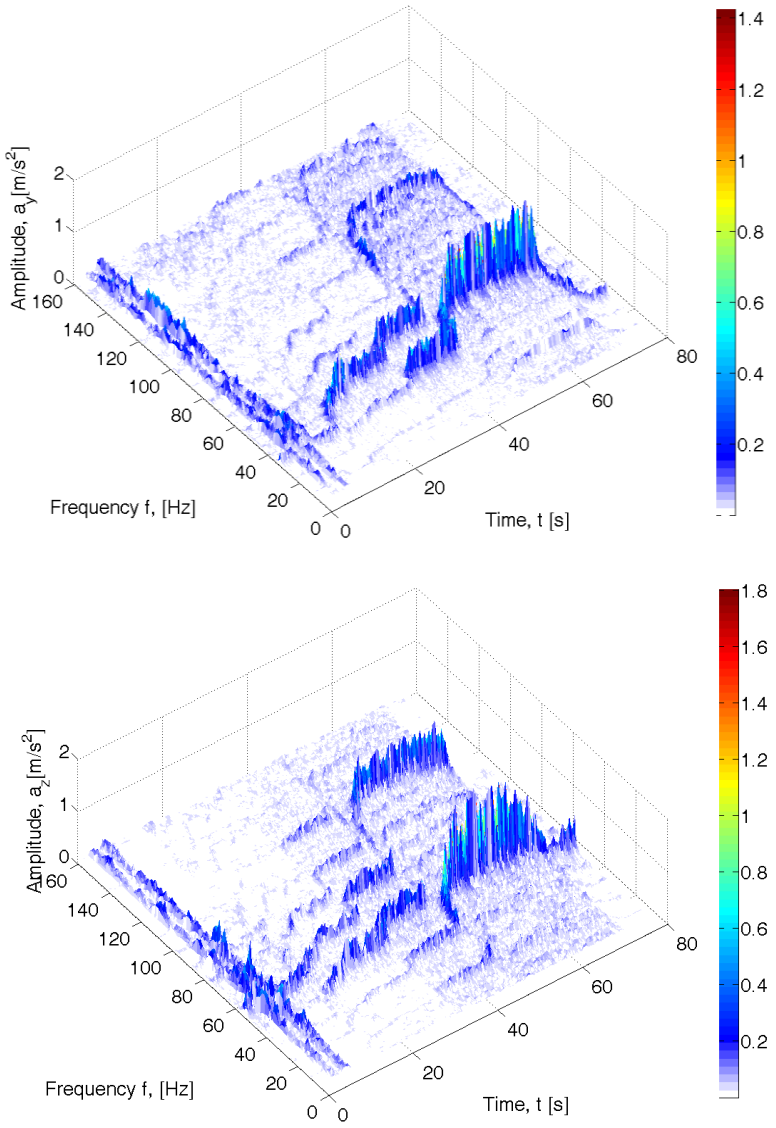

Figure 3. STFT spectrum for an faultless IC engine

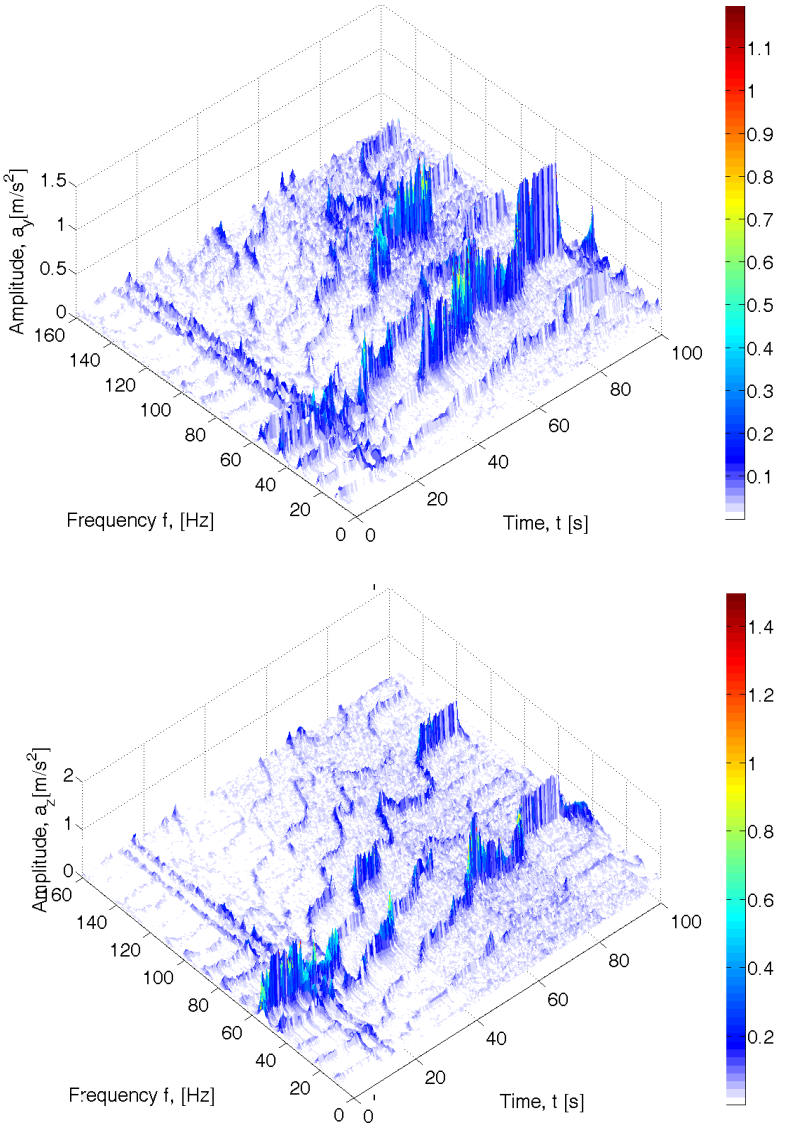

Figure 4. STFT spectrum for a malfunctioning IC engine - time gap in fuel injection

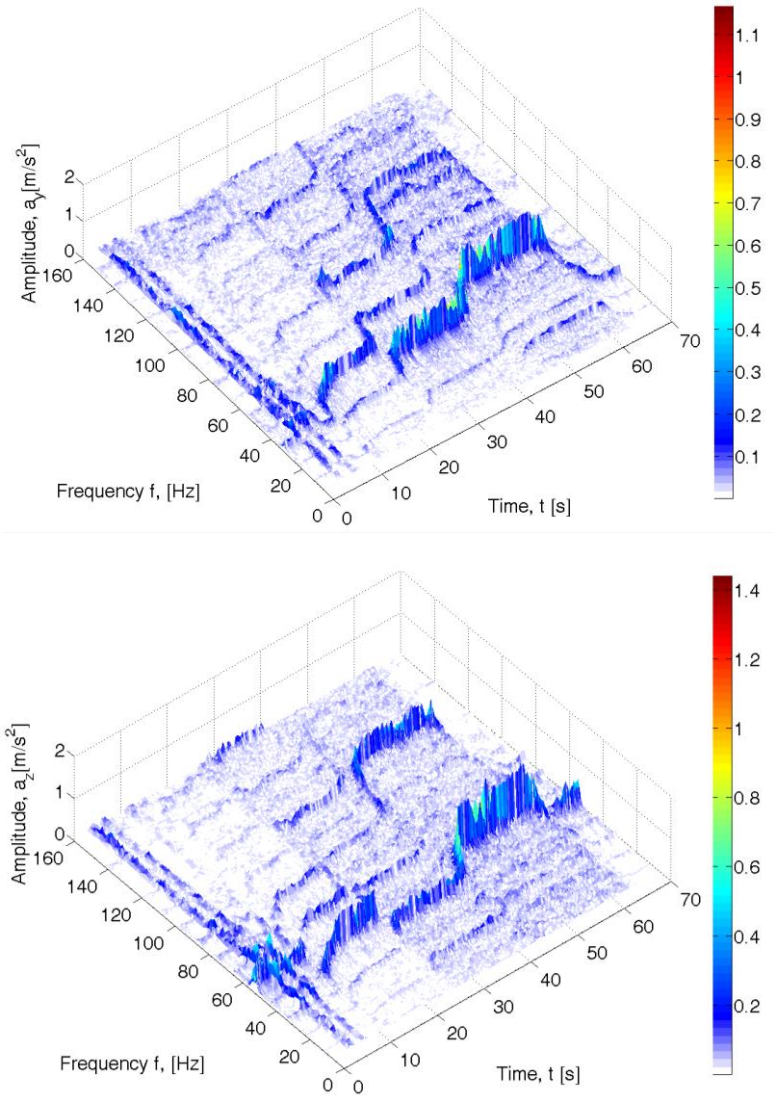

Figure 5. STFT spectrum for a malfunctioning IC engine - identified air leak in one of the cylinders

STFT waveforms (Fig. 3, 4, 5) show the bands of local amplitudes for the components of vehicle structure vibration acceleration for given engine speeds. The occurrence of dominant amplitudes depends on both the engine speed and the set defect (no injection, spark plug socket leakage). They provide an illustrative map of

changes in amplitudes in the spectrum as a result of changes in engine speed and the given failure.

For further analysis of the acceleration signal, waveforms were used at a constant rotational speed of the engine crankshaft. Fragments of the time series of recorded signals for the speeds of 1250 rpm and 3500 rpm are presented in Figures 6, 7. The waveforms of the vehicle acceleration signal have a periodic sinusoidal shape. The specified failure causes a change in the shape of the signal. This is particularly evident in the absence of injection at a speed of 1250 rpm (Fig. 6b). At 3500 rpm, the specified defects cause signal distortion and additional harmonics.

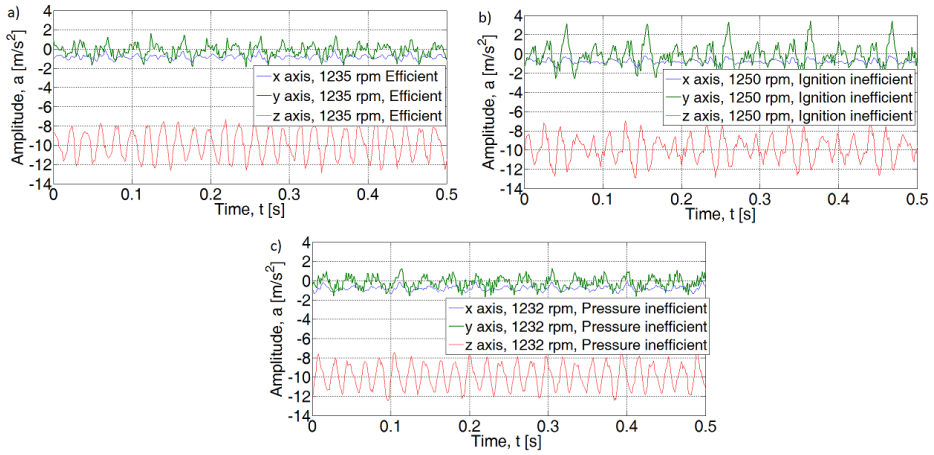

Figure 6. Acceleration sensor signal for 1250 rpm engine speed

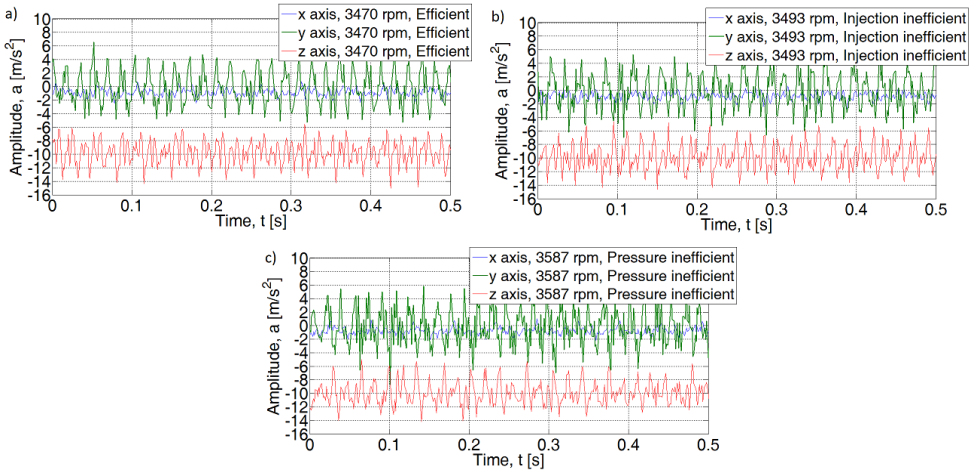

Figure 7. Acceleration sensor signal for 3500rpm engine speed

A fixed signal window value of 3 sec was adopted for the FFT transform. Then, for 1250 rpm, the acceleration signal was obtained, taking into account 31 cycles of each cylinder of the internal combustion engine (1 cycle = 2 shaft revolutions). Whereas for 3500 rpm the spectrum for 87 cycles of each cylinder.

For an efficient internal combustion engine at idle, the maximum acceleration values for the basic harmonic (f_1) are: a_x = 0.028 m/s^2, a_y = 0.11 m/s^2 and a_z = 0.13 m/s^2 (Fig. 8). The highest acceleration values for the efficient motor were obtained for subsequent folds of the basic harmonic: *y* axis ($f_{1.5}$) a_y = 0.5 m/s^2, and for the *z* axis ($f_{2.5}$) a_z = 1.05 m/s^2. Introduced defects in the form of lack of injection into one cylinder or leakage of the spark plug caused a visible increase in the value of amplitudes for individual axes. The amount of increase depends on the type of damage. In the case of an malfunction at injection system, an increase is seen for the *x* axis for harmonics: (f_1, f_2, $f_{2.5}$), for the *y* axis: f_1, f_2, $f_{2.5}$, f_3 and the *z* axis: f_2 and $f_{2.5}$ (Fig. 8). The introduction of a malfunction in the form of a leak in the connection of the spark plug with the head did not introduce changes in the analyzed spectrum.

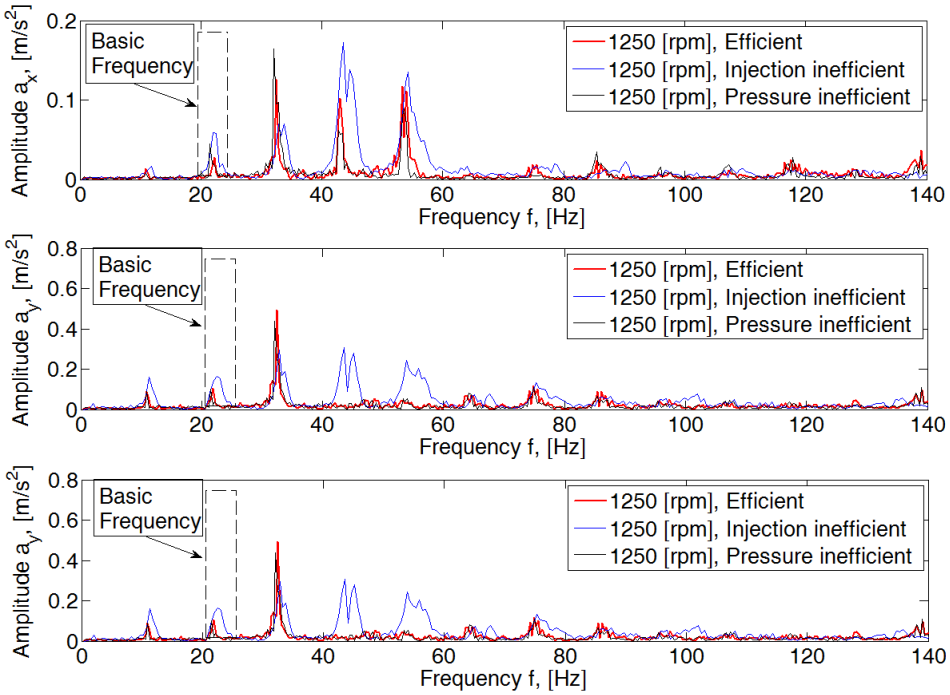

Figure 8. FFT spectral amplitude for 1250 rpm combustion engine

The increase in amplitude values is also visible for other engine speed ranges. An example of the course for the rotational speed of the crankshaft 3500 rpm is shown in Fig. 9.

Dominant amplitudes in the fundamental frequency range f_1 as well as $f_{1.5}$ and f_2 are visible in the analyzed spectrum. For an efficient motor, the amplitude values for f_1 are: a_x = 0.18 m/s^2, a_y = 1.89 m/s^2, and a_z = 0.48 m/s^2. An increase in the amplitudes of subsequent harmonics of the fundamental frequency (x axis and y axis) is also visible.

The introduced fault in the form of an inefficient injection system caused an increase in amplitude, which is visible for the harmonics $f_{1.5}$ and f_2 and f_1 for the z axis. The leakage of the candle results in an increase in the amplitudes of the x and y axis accelerations for the f_2 harmonic.

Based on the known rotational speed of the engine crankshaft, its basic frequency f_1 was determined using a frequency range window of +/- 1.5 Hz. Then dominant values of component acceleration amplitudes were determined for the n-order n = $f_{0.5}$; f_1; $f_{1.5}$; f_2; $f_{2.5}$. For the x axis, these values were determined as $a_{x0.5}$; a_{x1}; $a_{x1.5}$; a_{xn},

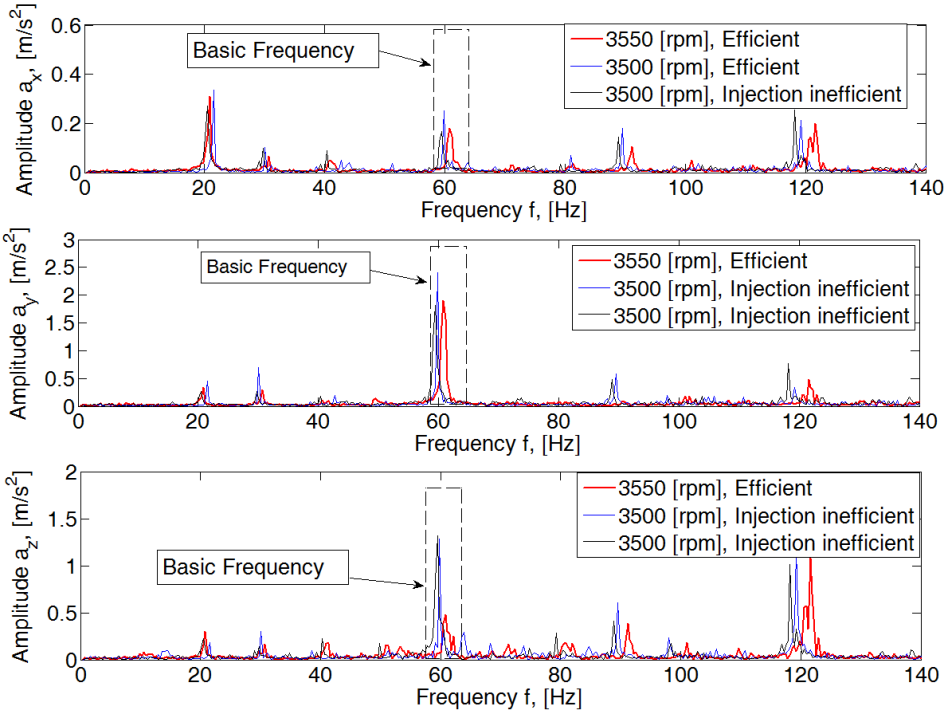

Figure 9. FFT spectral amplitude for 3500 rpm combustion engine

Then, relative values were determined for individual harmonics relative to the fundamental frequency. The obtained values take the designation A_{xn} (n-order of the analyzed basic harmonic) for individual harmonic components of the signal spectrum. Based on equation (3, 4, 5), the acceleration components for the measuring axis *x*, *y*, *z* were determined for the selected rotational speed of the internal combustion engine.

$$A_{xn} = \frac{a_{xn} \cdot 100}{a_{x1}} \tag{3}$$

$$A_{yn} = \frac{a_{yn} \cdot 100}{a_{y1}} \tag{4}$$

$$A_{zn} = \frac{a_{zn} \cdot 100}{a_{z1}} \tag{5}$$

Conditions have been adopted for individual residuals that determine the relationships for individual harmonics of the analyzed spectrum. The values obtained are relative to the value of the fundamental frequency signal.

Table 2. Residual specify in table for 1250 rpm

Nr resid.	Limit state ***WS***	Logical value ***MD*** of benchmark data for specified engine condition		
		faultless	Injection malfunction	Reduced compression pressure
1	$A_{x1.0} > A_{x0.5}$	$MD11 = 1$	$MD21 = 1$	$MD31 = 1$
2	$A_{x1.5} > A_{x1}$	$MD12 = 1$	$MD22 = 1$	$MD32 = 0$
3	$(A_{x1.5} + A_{x0.5}) > A_{x1}$	$MD13 = 1$	$MD23 = 0$	$MD33 = 0$
4	$A_{x2} > A_{x1.5}$	$MD14 = 1$	$MD24 = 1$	$MD34 = 1$
5	$A_{x2.5} > A_{x2}$	$MD15 = 1$	$MD25 = 1$	$MD35 = 0$

Table 3. Benchmark values of residual for 1250 rpm

Limit state ***WS***	Logical value ***ME*** for experimental data
$A_{x1.0} > A_{x0.5}$	$ME1$
$A_{x1.5} > A_{x1}$	$ME2$
$(A_{x1.5} + A_{x0.5}) > A_{x1}$	$ME3$
$A_{x2} > A_{x1.5}$	$ME4$
$(A_{x2.5}) > A_{x2}$	$ME5$

Table 4. IC engine identification table for 1250 rpm

Comparsion of readings (logical differential)	Logical value of state identification determinant ***WD***		
MD11⇔ME1	0 = compatible 1 = incompatible	0 = compatible 1 = incompatible	0 = compatible 1 = incompatible
MD12⇔ME2 →	…..		
MD13⇔ME3	…..		
MD14⇔ME4	…..		
MD15⇔ME5	…..		
	Percenta- geshare *WS* for *WD* = 0	Percenta- geshare *WS* for *WD* = 0	Percenta- geshare *WS* for *WD* = 0

This solution does not clearly indicate the type of fault, but the probability of its symptoms. The obtained largest percentage value of the *WD* = 0 group of determinants consistent with the adopted relations (*MD* = *ME*) testifies to the probability of occurrence of a given fault.

4. Identification matrix

Obtained experimental data was analyzed with the use of described method basing on diagnostic matrix to identify malfunctions of the research object. A working example was shown for experimental data obtained for an engine speed of 1250 rpm. Values of acceleration components for *x*, *y*, *z* axes, specific frequency ranges (in relation to base frequency) and assumed state of the engine were shown in Fig. 8. Relative values were then determined for this portion of experimental data.

Table 5. Data analysis for 1250 rpm in *x* axis

Nr resid.	*MDx*1	*MDx*2	*MDx*3	*MEx*		*WIx*1	*WIx*2	*WIx*3
1	1	1	1	1		0	0	0
2	1	1	1	1		0	0	0
3	1	1	1	1		0	0	0
4	0	1	0	1		1	0	1
5	1	0	1	0		1	0	1
					WSx [%]	60	100	60

Table 6. Data analysis for 1250 rpm in *y* axis

Nr resid.	*MDx*1	*MDx*2	*MDx*3	*MEx*		*WIx*1	*WIx*2	*WIx*3
1	1	1	1	0		1	1	1
2	1	1	1	1		0	0	0
3	1	1	1	1		0	0	0
4	0	1	0	1		1	0	1
5	1	0	1	0		1	0	1
					WSx [%]	40	80	40

Table 7. Data analysis for 1250 rpm in *z* axis

Nr resid.	*MDx*1	*MDx*2	*MDx*3	*MEx*		*WIx*1	*WIx*2	*WIx*3
1	1	1	1	1		0	0	0
2	0	0	1	0		0	0	1
3	1	0	1	0		1	0	1
4	0	1	0	1		1	0	1
5	0	1	1	1		0	0	0
					WSx [%]	60	100	40

Table 8. Data analysis for 3500 rpm in *x* axis

Nr resid.	*MDx*1	*MDx*2	*MDx*3	*MEx*		*WIx*1	*WIx*2	*WIx*3
1	1	1	1	0		1	1	1
2	0	0	0	1		1	1	1
3	0	1	1	1		1	1	0
4	1	1	1	1		0	0	0
5	0	1	0	0		0	1	0
					WSx [%]	40	40	60

Table 9. Data analysis for 3500 rpm in *y* axis

Nr resid.	*MDx*1	*MDx*2	*MDx*3	*MEx*		*WIx*1	*WIx*2	*WIx*3
1	1	1	1	0		1	1	1
2	0	0	0	1		1	1	1
3	0	0	0	1		1	1	1
4	1	0	1	0		1	0	1
5	0	1	0	0		0	1	0
					WSx [%]	20	20	20

Table 10. Data analysis for 3500 rpm in *z* axis

Nr resid.	*MDx*1	*MDx*2	*MDx*3	*MEx*		*WIx*1	*WIx*2	*WIx*3
1	1	1	1	1		0	0	0
2	0	0	0	0		0	0	0
3	1	0	0	1		0	1	1
4	1	1	1	1		0	0	0
5	0	0	0	0		0	0	0
					WSx [%]	100	80	80

Benchmark data for diagnostic matrices *MDx*, *Mdy*, *MDz* (Tables 5-10) was obtained basing on the analysis of acceleration components and engine condition.

The determinants of the relationship (residuy) of particular harmonic axes *x*, *y*, *z* for the efficient engine were marked in columns: *MDx*1, *Mdy*1, *MDz*1. For engine with damaged injection *MDx*2, *MDy*2, *MDz*2. For a motor with a non-sealed combustion chamber: *MDx*3, *MDx*3, *MDx*3. The markers of the analyzed signal were denoted as: *MEx*, *MEy*, *MEz*.

The individual *MDn* reference data were compared with resi - des of the tested *MEn* signal, obtaining information on existing relations. In the case of compliance (e.g. *MDx*1 (1) and *MEx* (1)) for 1250 rpm (Tab. 4), the value of *WIx*1 (1) is 0. In the case of non-compliance (eg *MDx*1 (2) and *MEx* (2)), the value of *WIx*1 (2) is 1.

By analyzing specific measurement data for the engine, a percentage probability of its state was obtained. Data analysis for identified malfunctions in the form of time gap in fuel injection and air leak in one of engine cylinders is shown in Tables. 5, 6, 7. Show case data analysis for 1250 rpm, whereas Tables 8, 9, 10 show data analysis for 3500 rpm.

Identification matrices allow to identify time gap in fuel injection with 100%, 83%, 100% in *x*, *y*, *z* axes, and an air leak within the engine cylinder with 67%, 50%, 50% probability (in *x*, *y*, *z* axes) for 1250 rpm. For the analyzed signal, the greatest probability of engine failure was defined as pressure damage. For increased engine speed (3500 rpm), there are lower signal distortion. As a result, identifying malfunctions based on the presented diagnostic matrix is more difficult, and the accuracy of decisions is burdened with a significant error. It is therefore necessary to develop a relationship for comparing harmonics for individual characteristic speeds of an internal combustion engine.

5. Conclusions

The presented research has shown that it is possible to identify engine malfunctions by analyzing the harmonic components of vehicle chassis vibrations with the use of residuals. Two distinct engine failures were purposefully introduced to an investigated spark-ignition engine mounted in RZR 1000 ATV- time gap in fuel injection and air leak in engine cylinder. The tests were carried out for various engine speeds without additional load.

In the area of low frequencies, it was observed that the specified engine failure (no injection or damage to one of the cylinders) causes a change in the amplitude of vibration accelerations for a frequency corresponding to 0.5; 1; 1.5; 2 and 2.5 engine speeds f_o.

Analysis of the relative values of the components of harmonic amplitudes noted differences in spectral lines resulting from malfunction of the engine. This allowed the authors to formulate a reasoning matrix for identifying engine failure basing on comparative analysis of harmonic components. In future research, it would seem beneficial to conduct a similar analysis of harmonic components for different engine speeds and to specify a diagnostic criterion.

In the developed diagnostic matrix to identify the malfunction of the internal combustion engine based on the vibration of the vehicle structure, changes in the amplitudes of the individual harmonics of the signal in the spectrum were used.

This solution is an alternative to diagnostic inference in real vehicle operation conditions, due to the easy installation of the sensor. It should be noted, however, that the measurement is indirect, and the results presented do not take into account the effect of dissipative elastic elements of engine mounting to the vehicle structure. This compaction is a further part of the work carried out as part of the vehicle vibration analysis in terms of safety and comfort, and early identification of damage.

References

1. J. A. Wajand, J. T. Wajand, *Medium and high speed piston internal combustion engines* (in Polish), WNT, Warsaw 2000.
2. J. Grajales, H. Quintero, J. López, C. Romero, E. Henao, O. Cardona, *Engine diagnosis based on vibration analysis using different fuelblends*, Diagnostic **18**(4) (2017) 27 – 36.
3. J. A. Grajales, H. F. Quintero, C. A. Romero, E. Henao, J. F. López, D. Torres, *Combustion pressure estimation method of a spark ignited combustion engine based on vibration signal processing*, Journal of Vibroengineering, **18**(7) (2016) 4237 – 4247.
4. A. Taghizadeh-Alisaraei, A. Mahdavian, *Fault detection of injectors in diesel engines using vibration time-frequency analysis*, App. Acoustics, **143** (2019) 48 – 58.
5. J. Flett, G. M. Bone, *Fault detection and diagnosis of diesel engine valve trains*, Mech. Sys. and Sig. Proc., **72-73** (2016) 316 – 327.
6. Z. Geng, J. Chen, J. B. Hull, *Analysis of engine vibration and design of an applicable diagnosing approach*, Int. J of Mech. Sciences, **45**(8) (2003) 1391 – 1410.
7. M. Ettefagh, M. Sadeghi, V. Pirouzpanah, H. Arjmandi Tash, *Knock detection in spark ignition engines by vibration analysis of cylinder block: A parametric modeling approach*, Mech. Sys. and Sig. Proc., **22** (2008) 1495 – 514.
8. S. Delvecchio, P. Bonfiglio, F. Pompoli, *Vibro-acoustic condition monitoring of Internal Combustion Engines: A critical review of existing technique*, Mech. Sys. and Sig. Proc., **99** (2018) 661 – 683.
9. R. Sroka, *Determining the impact of switching off ZI engine cylinders on changes in the engine's vibroacoustic signal* (in Polish), Transport, Silesian University of Technology 2008.
10. R. Burdzik, *Research on the influence of engine rotational speed to the vibration penetration into the driver via feet - multidimensional analysis*, J of Vibroeng., **15**(4) (2013) 2114 – 2123.
11. J. Dziurdź, *Analysis of nonlinear phenomena in the diagnosis of vehicle propulsion systems* (in Polish), Warsaw-Radom 2013.
12. K. Jafarin, M. Mobin, R. Jafari-Marandi, E. Rabiei, *Misfire and valve clearence faults detaction in the combustion engines based on a multi- sensor vibration signal monitoring*, Measurement, **128** (2018) 527 – 536.

13. K. Prażnowski, J. Mamala, *Problems in Assessing Pneumatic Wheel Unbalance of a Passenger Car Determined with Test Road in Normal Conditions*, SAE Tech. Pap., Grand Rapids 2017.
14. K. Prażnowski, J. Mamala, *Classification of the road surface condition on the basis of vibrationsof the sprung mass in a passenger car*, IOP Conference Series: Mat. Scienc. and Engineering, Zakopane 2016.
15. J. Korbicz, J. Kościelny, Z. Kowalczuk, W. Cholewa, *Process diagnostics, Models, artificial intelligence methods, applications* (in Polish), WNT Warszawa 2002.